



# Ascorbyl stearate stimulates cell death by oxidative stress-mediated apoptosis and autophagy in HeLa cervical cancer cell line in vitro

Shirish Dinkar Mane<sup>1</sup> · Akhilender Naidu Kamatham<sup>1</sup>

Received: 4 June 2018 / Accepted: 10 February 2019 / Published online: 2 March 2019  
© King Abdulaziz City for Science and Technology 2019

## Abstract

In this study, Asc-s was evaluated for anti-cancer effect using cervical cancer cells (HeLa). Results determine that Asc-s treatment-induced dose-dependent inhibition of proliferation of HeLa cells and induced apoptosis. Flow-cytometry analysis shows Asc-s treatment-induced accumulation of cells at sub-G0/G1 stage of cell cycle and induced apoptosis as confirmed by DAPI, propidium iodide, and acridine staining in HeLa cells. Asc-s entered the cells and metabolized to ascorbate and stearate moieties, increased membrane permeability, and decreased membrane fluidity in HeLa cells. Asc-s treatment-induced dose-dependent increase in autophagy protein LC3-II, mRNA levels and decreased Nrf-2 levels in HeLa cells. It is hypothesized that both ascorbyl radical and stearyl moieties of Asc-s induced cytotoxicity by generating reactive oxygen species (ROS) and modulating membrane fluidity/permeability leading to apoptosis/autophagy of HeLa cells. Thus, our findings demonstrate that Asc-s as anti-proliferative and apoptosis inducing compound in cervical cancer cells.

**Keywords** Ascorbyl stearate · HeLa cancer cells–anti-proliferation · Autophagy/ apoptosis · Liquid chromatography · Gas chromatography

## Introduction

Cancer is one of the major disorder and a public health concern worldwide. Current data from the National Cancer Registry Program (NCRP) indicate that the most common sites of cancer among women are the breasts and the cervix (Nandakumar et al. 2009). Cervical cancer is the most common malignancy and second leading cause of death in women aged 19–39 years (Jemal et al. 2011). Every year in India, about 122,844 women are diagnosed with cervical cancer and 67,477 die from the disease (Bruni et al. 2015). Invasive cervical cancer incidence and mortality is one of the major issues in the developed and developing countries. Molecular studies have shown that HPV-16 and 18 are the two most common oncogenic types found in invasive cervical cancer, and out of these two HPV-16 have been found more commonly in cervical cancer patients (Bhatla et al. 2008). Cervical cancer patients (~35%) treated with

radiation are likely to develop persistent and metastatic form of the disease (Mountzios et al. 2013).

L-Ascorbic acid as an anti-cancer agent was recognised long ago in 1970s; however, randomized controlled clinical trials produced inconsistent results due to poor bioavailability and reduced efficacy of ascorbic acid (Wilson et al. 2014). Despite the ambiguity on anti-cancer propensity of ascorbic acid, a number of studies were undertaken to study the effect of ascorbic acid on various malignant cell lines (Shibuya et al. 2012; Roberts et al. 2015). However, its susceptibility to thermal and oxidative degradation, together with its poor lipo-solubility and kidney excretion, makes it difficult to maintain milli molar concentrations in blood (Levine et al. 1996). To solve these issues, a number of novel ascorbic acid derivatives have been developed by modifying hydroxyl groups of vitamin C. Among them, fatty acid esters of ascorbic acid namely ascorbyl palmitate and ascorbyl stearate, have attracted considerable interest as anti-cancer compounds due to their lipophilic nature and easy passage across cell membranes and blood brain barrier (Sawant et al. 2011). We have earlier reported that ascorbyl stearate inhibits proliferation and induces apoptosis in human glioblastoma, pancreatic, and human ovarian cancer cells. Ascorbyl stearate treatment inhibited cancer cell growth by interfering

✉ Akhilender Naidu Kamatham  
aknaidu@cftri.res.in; akhilnaidu@gmail.com

<sup>1</sup> Department of Biochemistry, CSIR-Central Food Technological Research Institute, 570020 Mysore, India

with cell-cycle progression, clonogenicity, induced apoptosis by modulating signal transduction pathways of IGF-IR/p53/p21/cyclins (Naidu et al. 2007). In this study, we report the possible mechanism of cell death induced by ascorbyl stearate by interfering with cell cycle at sub-G0/G1 stage of cell cycle, modulating membrane permeability and fluidity, increasing ROS levels, decreasing Nrf-2 levels in HeLa cervical cancer cells.

## Materials and methods

### Chemicals

Ascorbyl stearate (Asc-s) was purchased from Tokyo Chemical Industry (TCI), Japan. Cell-culture grade plastic wares and chemicals such as enhanced chemiluminescence (ECL) kit were purchased from Himedia, Bangalore and Life technologies, Bangalore. Cell-culture grade chemicals such as dimethyl sulphoxide (DMSO), acridine orange (AO), propidium iodide (PI), boron trifluoride in methanol, 1,6-diphenyl-1,3,5-hexatriene (DPH), 4',6-diaminidino-2-phenylindole (DAPI), and other analytical reagents were obtained from Sigma Chemicals, Bangalore. Carboxy-fluoresceinsuccinimidyl ester (CFSE) cell proliferation kit was obtained from Thermo Fisher, Mumbai. HPLC grade chemicals were purchased from Sisco Research Laboratory, Bangalore. Cell permeable trolox (TRO) was procured from Calbiochem (USA). Halt protease inhibitor cocktail, Bicinchoninic acid (BCA) kit for protein assay was procured from Thermo Fisher Scientific, Bangalore. Rabbit anti—LC3 antibody and Rabbit anti—beta actin antibody as well as HRP—conjugated anti-rabbit, IgG antibody were purchased from Cell Signaling Technology, Bangalore and Abcam, Kolkata, respectively. Polyvinylidene fluoride (PVDF) membrane was purchased from Pall Corporation, Bangalore.

### Cell culture

HeLa cells were obtained from national cell line repository at National Centre for Cell Science (NCCS), Pune. HeLa cells were cultured in Dulbecco's modified eagle's medium (DMEM) supplemented with 10% foetal bovine serum (FBS) at 37 °C in 5% CO<sub>2</sub>. Cells were plated at least 48 h before drug treatment.

### Ascorbyl stearate (Asc-s) preparation

Asc-s was dissolved in DMSO and 1 mM stock DMEM/Asc-s concentration was prepared by adjusting the pH to 7 with 0.1 mM sodium hydroxide in sterilised Milli Q (MQ) water.

### Effect of Asc-s on HeLa cell proliferation

The effect of Asc-s on HeLa cell growth was evaluated by 3-(4,5-dimethylthiazol-2-yl)-2,5-diphenyltetrazolium bromide (MTT) assay (Naidu et al. 2007). In brief,  $2 \times 10^4$  HeLa cells were seeded in 96 well plates in 0.15 ml DMEM. HeLa cells were treated with Asc-s at concentration of 0, 50, 100, 150, 200, 300  $\mu$ M and DMSO as vehicle control. After 48 h, cell proliferation and viability was determined by MTT assay and absorbance was read at 570 nm using microplate reader (Biorad, California). A separate experiment showing linear relation between absorbance of MTT and HeLa cell was verified with a correlation coefficient of 0.99. The decrease in absorbance is commensurable with loss of cell viability.

### Cell proliferation by CFSE labelling

The dye dilution method was adopted in determining cell proliferation by Flow cytometer (Sharma et al. 2010). HeLa cells were labelled with CFSE (20  $\mu$ M, 5 min, 37 °C), washed three times with DMEM. The cells were plated and treated with Asc-s at concentration of 0, 50, 100, 150, 200 and 300  $\mu$ M with DMSO as vehicle control. After 48 h of treatment, HeLa cells were harvested and cell proliferation was measured using flow cytometer (Partec, Germany). CFSE, a non-fluorescent dye, taken up by both live and dead cells is converted to fluorescent derivative carboxy fluorescein, an amino group binder in cellular proteins by the live cell's esterase enzymes. Percent daughter cells were calculated by gating the cells with decreased CFSE fluorescence as compared to undivided cells using Flowjo software (treestarinc).

### Cell-cycle analysis by flow cytometry

HeLa cells treated with 0, 50, 100, 150, 200, and 300  $\mu$ M of Asc-s for 48 h were subjected to flow cytometry to detect cell cycle and measure apoptosis by analysing cells with a DNA content less than 2n ("sub-G1 cells") (Trumpi et al. 2015). Cells harvested were incubated in PBS buffer + 0.1% Triton-X + 0.1% sodium citrate (pH 7.4), supplemented with 50  $\mu$ g/ml PI overnight at 4 °C. Cell analysis was performed using Flow cytometer (Partec, Germany). The PI fluorescence signal at FL3-PI versus histogram was used to determine sub-G1 and cell-cycle distribution by Flowjo software.

### Detection of apoptosis by DAPI, propidium iodide and acridine orange staining

HeLa cells were treated with Asc-s at 126  $\mu$ M for 24 h and 48 h. After incubation period, cells were stained with DAPI

for 30 min at 37 °C in dark. Cells were visualized under a fluorescent microscope. Cells with nuclei containing clearly condensed chromatin or cells with fragmented nuclei were inferred as apoptotic cells (Rabelo et al. 2012).

Apoptosis assay was performed by dual staining of PI and AO as described earlier (Wahab et al. 2009). In brief HeLa cells ( $1 \times 10^4$  cells/well) were treated with Asc-s at 126  $\mu\text{M}$  for 24 h and 48 h. Asc-s and vehicle treated HeLa cells were incubated with AO followed by PI for 5 min. The cells were observed under the microscope, the cells stained green with AO were viable cells and the nuclei stained orange with PI were considered as apoptotic cells.

### Measurement of ROS in HeLa cells

The dye dichlorofluorescein diacetate DCFH<sub>2</sub>-DA, which is oxidized to fluorescent DCF by hydroperoxides, was used to measure reactive oxygen species (ROS). Intracellular ROS in HeLa cells was measured by spectrofluorimetry method (Patwardhan et al. 2013). HeLa cells were incubated with 20  $\mu\text{M}$  (DCF-DA) for 25 min at 37 °C, followed by treatment of cells with different concentrations of Asc-s (50–200  $\mu\text{M}$ ) for 15–60 min. ROS scavenger cell permeable trolox (100  $\mu\text{M}$ ) treated to cells with Asc-s 126  $\mu\text{M}$  for 15–60 min was also used as control. The changes in fluorescence resulting from oxidation of H<sub>2</sub>DCF to DCF were measured at an excitation wavelength of 485 nm and an emission wavelength of 530 nm using a spectrofluorimeter.

### Electrophoretic mobility-shift assay (EMSA)

HeLa cells were exposed to 25–200  $\mu\text{M}$  Asc-s or 126  $\mu\text{M}$  Asc-s for 0–6 h and were harvested after 4 h for nuclear pellets as described earlier (Patwardhan et al. 2013). EMSA was performed by Nrf-2 oligonucleotide (5'-TGGGGAACCTGTGCTGATCACT GGAG-3') in the presence of 0.5  $\mu\text{g}$  of poly(2'-deoxyinosinic-2'-deoxycytidylic acid) in binding buffer (25 mM Hepes, pH 7.9, 0.5 mM EDTA, 0.5 mM DTT, 1% NP-40, 5% glycerol, and 50 mM NaCl) for 30 min at 37 °C. The DNA–protein complex formed was separated from free oligonucleotide on 6.6% native polyacrylamide gels using buffer containing 50 mM Tris, 200 mM glycine, and 1 mM EDTA, pH 8.5. The dried gel was exposed to a phosphor image plate and the radioactive bands were visualized using a phosphor image plate scanner (Amersham Biosciences, USA).

### Measurement of membrane permeability of HeLa cells

Measurement of membrane permeability of HeLa cells on treatment with Asc-s was carried out as per the method described (Lu et al. 2010). HeLa cells ( $0.1 \times 10^6$ ) were

treated with different concentration of 0, 50, 100, 150, 200, and 300  $\mu\text{M}$  of Asc-s and DMSO as vehicle control for 48 h, the cells were collected, counted and incubated with 100 ng PI for 30 min at 4 °C. Samples were washed in Dulbecco's modified phosphate buffered saline (DPBS) and then resuspended for fluorescence analysis in fluorescence spectrophotometer (Shimadzu RF 5301, Japan). Fluorescence intensity was calculated as  $F_{\text{sample}}/F_{\text{CK}}$ , where  $F_{\text{sample}}$  and  $F_{\text{CK}}$  are the intensities of the sample and control, respectively.

### Measurement of membrane fluidity of HeLa cells

Measurement of membrane fluidity of HeLa cells on treatment with Asc-s was carried out as per the method described (Lu et al. 2010), with slight modification. HeLa cells ( $0.1 \times 10^6$ ) treated with Asc-s at a concentration of 0, 50, 100, 150, 200, and 300  $\mu\text{M}$  for 48 h along with DMSO as vehicle control were harvested, counted, and incubated with 1,6-diphenyl-1,3,5-hexatriene (DPH) for 15 min at room temperature in dark for incorporation of probe into membranes. Fluorescence measurements were acquired on fluorescence spectrophotometer (Shimadzu RF 5000, Japan) at 360 and 450 nm as excitation and emission wavelengths, respectively. The degree of fluorescence anisotropy ( $r$ ) was estimated.

### Estimation of Asc-s and its metabolites in HeLa cells

HeLa cells ( $1 \times 10^6$ ) were treated with 126  $\mu\text{M}$  Asc-s for 12 h, 24 h, and 48 h, and the cells were homogenized and subjected to reverse phase HPLC to detect intracellular ascorbyl stearate (Cleaver 2015). The cell homogenate was centrifuged at 12,000 rpm for 15 min at 4 °C. An aliquot of filtrate was injected on octadecyl-silica column (Supelco, Sigma-Aldrich, US) (250 mm, 5-micron), and the mobile phase was methanol: acetonitrile: formic acid (1%) (50: 47.5: 2.5) with a flow rate of 1 ml/min. Asc-s was detected with evaporative light scattering detector (ELSD) (Waters, US). AA, Asc-s, and stearic acid (SA) were resolved with a retention time of 2.04 min, 4.3 min, and 5.59 min, respectively, under employed chromatographic conditions. The concentrations of AA, Asc-s, and SA were estimated by the standard plots developed using the standards.

### Fatty acid analysis of HeLa cells

HeLa cells ( $1 \times 10^6$ ) treated with Asc-s at 126  $\mu\text{M}$  for 12, 24, and 48 h were collected by centrifugation at  $1500 \times g$  for 5 min, and the total lipids were methylated with 40% boron trifluoride in methanol to obtain fatty acid methyl esters (FAMES) (Folch et al. 1957; Morrison and Smith 1964). Fatty acid analysis was carried out in gas liquid chromatograph (Shimadzu GC-2010, Japan) with flame ionization

detector (FID) in isothermal conditions. The operating conditions were as follows: column temperature 220 °C, injection temp 230 °C and detector temp 240 °C. Nitrogen was used as the carrier gas. Individual fatty acids were identified by comparing with the retention times of reference fatty acid standards (Nu-Check Prep, Inc., USA) quantified by Shimadzu inbuilt software. The results are presented as relative percentage peak area of individual fatty acids.

### Immunoblot analysis of LC3 in HeLa cells

HeLa cells treated with Asc-s at a concentration of 0, 50, 100, 150, and 200 µM for 48 h along with DMSO as vehicle control were lysed in Radio-immunoprecipitation assay buffer (RIPA) buffer: 50 mM Tris-HCl, pH 7.4, 1% NP-40, 0.5% Sodium deoxycholate, 0.1% SDS, 150 mM NaCl, 2 mM EDTA with 1X protease inhibitor cocktail. Protein contents of cell lysates were determined by BCA kit and equal amount of protein (25 µg) were electrophoresed on 12% SDS-PAGE and wet transferred on methanol pre-activated PVDF membrane. Membranes were blocked with 5% non-fat milk powder and afterwards incubated for overnight at 4 °C with rabbit anti-LC3 antibody or rabbit anti-β-actin antibody as loading control and finally incubated with HRP-conjugated anti-rabbit, IgG antibody followed by exposure to ECL detection reagents and image capturing in Syngene G:Box unit. Densitometric analysis was performed using inbuilt syngene tools electrophoresis analysis software.

### Quantitative reverse transcription-PCR (real-time RT-qPCR) of LC3-II and Nrf-2

Total RNA was purified from HeLa cells treated with Asc-s along with DMSO as vehicle control using RNA purification kit. Nrf-2 levels were investigated in HeLa cell treated with Asc-s (0–150 µM) for 6 h and HeLa cell treated with 126 µM Asc-s for 0–6 h to corroborate the results with Nrf-2 EMSA profile, whereas LC3 levels were determined in HeLa cell treated with 0–200 µM Asc-s at 48 h. A 1 µg was employed for cDNA synthesis using verso cDNA synthesis kit; reaction mixtures of 20 µL was prepared with SYBR green master mix using Biorad CFX real-time PCR with primers as: GAPDH: primer 1, 5'-ACAAC TTTGGTATCG TGGAAGG-3' and primer 2, 5'-GCCATCACGCCACAG TTTC-3'; MAP1 LC3A: primer 1, 5'-CGTCCTGGACAA GACCAAGT-3' and primer 2, 5'-CTCGTCTTT CTCCTG CTCGT-3' 22; (Kar et al. 2009) and Nrf2: primer 1, 5'-AGT GGATCTGCCAACTACTC-3' and primer 2, 5'-CATCTA CAAAC GGAATGTCTG-3' (Clements et al. 2006).

The amplification parameters were as follows: initial denaturation at 95 °C for 5 min prior to 39 thermal cycles of 95 °C for 15 s, 55 °C for 30 s, and 72 °C for 30 s, with the final extension of 65 °C for 5 min. Standard PCR reactions

were performed with 39 cycles. The PCR products were analysed and calculated by inbuilt Biorad software for fold expression levels, normalized to GAPDH, respective to samples.

### Effect of Asc-s on murine splenic lymphocytes

Effect of Asc-s was determined by treating murine splenic lymphocytes with Asc-s at concentration of 0–200 µM. In brief, splenic lymphocytes were isolated from C57BL/6 mice as mentioned by Checker et al. (2010). Cells were plated and incubated with Asc-s. After incubation of 24 h, cells were harvested and stained with 50 µg/ml PI (Lu et al. 2010) and acquired on high content screening instrument (Acumen Celistra) from TTP Labtech, UK.

### Statistical analysis

Statistical analysis was performed by one-way analysis of variance (ANOVA) and Dunnett test by comparing control with Asc-s-treated cells at different doses and time intervals using Graphpad statistical software (Graph pad instat).

## Results

### Asc-s inhibits proliferation of HeLa cells

HeLa cells incubated with different concentration of Asc-s (0, 50, 100, 150, and 200 µM) resulted in significant inhibition of cell growth. A dose-dependent inhibition curve was recorded, as shown in Fig. 1a ( $p < 0.001$ ). The maximal inhibition of cell proliferation was noted at Asc-s concentration of 200 µM, where in only 10% viability was seen when compared to control HeLa cells. IC<sub>50</sub> of Asc-s for 48 h was determined to be 126 µM by ED50 Plus v1.0, online software.

The anti-proliferative effect of Asc-s was also evinced from dose-dependent (0, 50, 100, 150, and 200 µM) inhibition of CFSE dye dilution in HeLa cells. The overlaid flow cytometric histograms were used to calculate percent daughter cells. Figure 1b–h shows per cent daughter cells when HeLa cells were exposed to different concentrations of Asc-s. Asc-s dose-dependently inhibited proliferation HeLa cells (% daughter cells  $74.4 \pm 0.7\%$ ,  $62.8 \pm 0.8\%$ ,  $25.5 \pm 0.9\%$ , and  $9.3 \pm 0.8\%$  at 50–200 µM of Asc-s treatment, respectively, as compared to  $80.3 \pm 0.6\%$  daughter cells in control group).

### Effect of Asc-s on cell cycle of HeLa cells

HeLa cells were cultured in the presence of Asc-s (0, 50, 100, 150, and 200 µM) for 48 h, stained with PI and cell cycle/apoptosis was measured by flow cytometry. As shown in Fig. 2a–e, a significant ( $p < 0.0001$ ) accumulation of cells



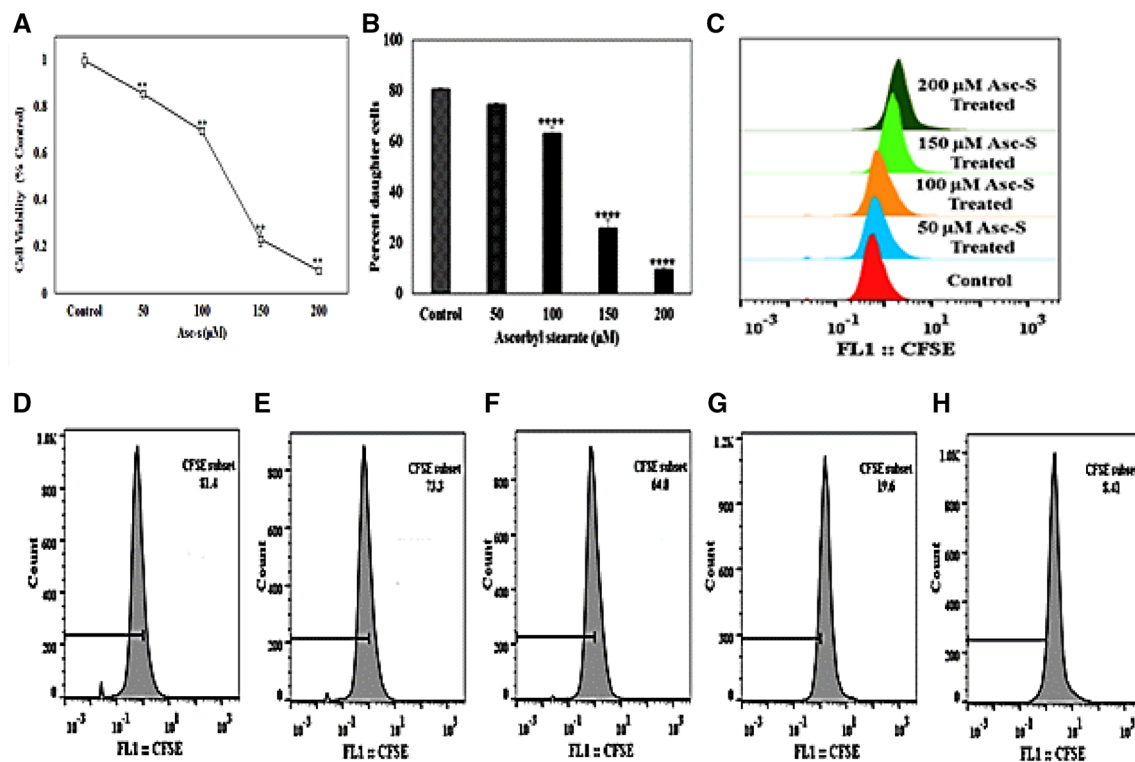


**Fig. 1** **a** Effect of different concentrations of Asc-s on viability of HeLa cells determined by MTT assay. A dose-dependent decrease in cell viability was observed on treatment with Asc-s. **b, c** Percent daughter cells of HeLa estimated by CFSE dye method at different concentrations of Asc-s treatment. **d–h** CFSE profile of HeLa cells

treated with 0, 50, 100, 150, and 200 µM Asc-s for 48 h. A significant dose-dependent decrease in CFSE counts was observed in HeLa cells on treatment with 50, 100, 150, 200 µM Asc-s. Data represent mean  $\pm$  SE ( $n=3$ ). Values are significant at  $**p < 0.01$ ,  $***p < 0.0001$

at sub-G0/G1 stage of cell cycle was observed in all doses of Asc-s treatment. Figure 2f shows the per cent cells in different phases of cell cycle at different doses of Asc-s treatment and apoptotic cells. HeLa cells showed a dose-dependent increase in percent apoptotic cells (sub G0/G1 peak) and a concomitant decrease in cells in G1 phase. The percentage of actively dividing cells in S/G2-M phases of cell cycle was also significantly suppressed by Asc-s in HeLa cells.

### Asc-s treatment-induced apoptosis in HeLa cells

HeLa cells treated with 126 µM Asc-s for 24 and 48 h were stained with DAPI and photographed under a fluorescence microscope. The results indicated that untreated cells had homogeneous nuclei (Fig. 3a), whereas Asc-s-treated cells exhibit condensed nuclei and apoptotic bodies with increase in time intervals (Fig. 3b, c).

Cells stained with PI and AO showed distinct morphological changes as indicated by nuclear degradation and nuclear asymmetric distribution in cells (Fig. 3d, g). Nuclear fission and cell disruption were manifested in Asc-s treated cells implying cell death (Fig. 3e, f, h, i).

### Asc-s modulates intracellular ROS levels

A significant increase in DCF (dichlorodihydrofluorescein) fluorescence was observed in 15 min of 150 and 200 µM of Asc-s treatment. The increase in ROS levels continued over 30 and 60 min, respectively, at higher doses of Asc-s treatment (Fig. 4). ROS levels were approximately the same when compared to untreated control and trolox treated control highlighting ROS generation by free oxygen radicals rather than reaction of Asc-s with DCF.

### Electrophoretic mobility-shift assay (EMSA) and RT-qPCR for Nrf-2

Nuclear translocation of Nrf-2 was assessed by EMSA (Fig. 5) at concentration dependent and time-dependent manner. HeLa cells showed higher levels of Nrf-2 in nuclear extracts, suggesting that Nrf-2 is constitutively active. Incubation with Asc-s abrogated nuclear translocation of Nrf-2. RT-qPCR analysis of Asc-s treated HeLa cell lysate showed ~60–70% decrease in Nrf-2 mRNA expression with respect to control cells, in a dose-dependent and time-dependent experiments ( $p < 0.05$ ).

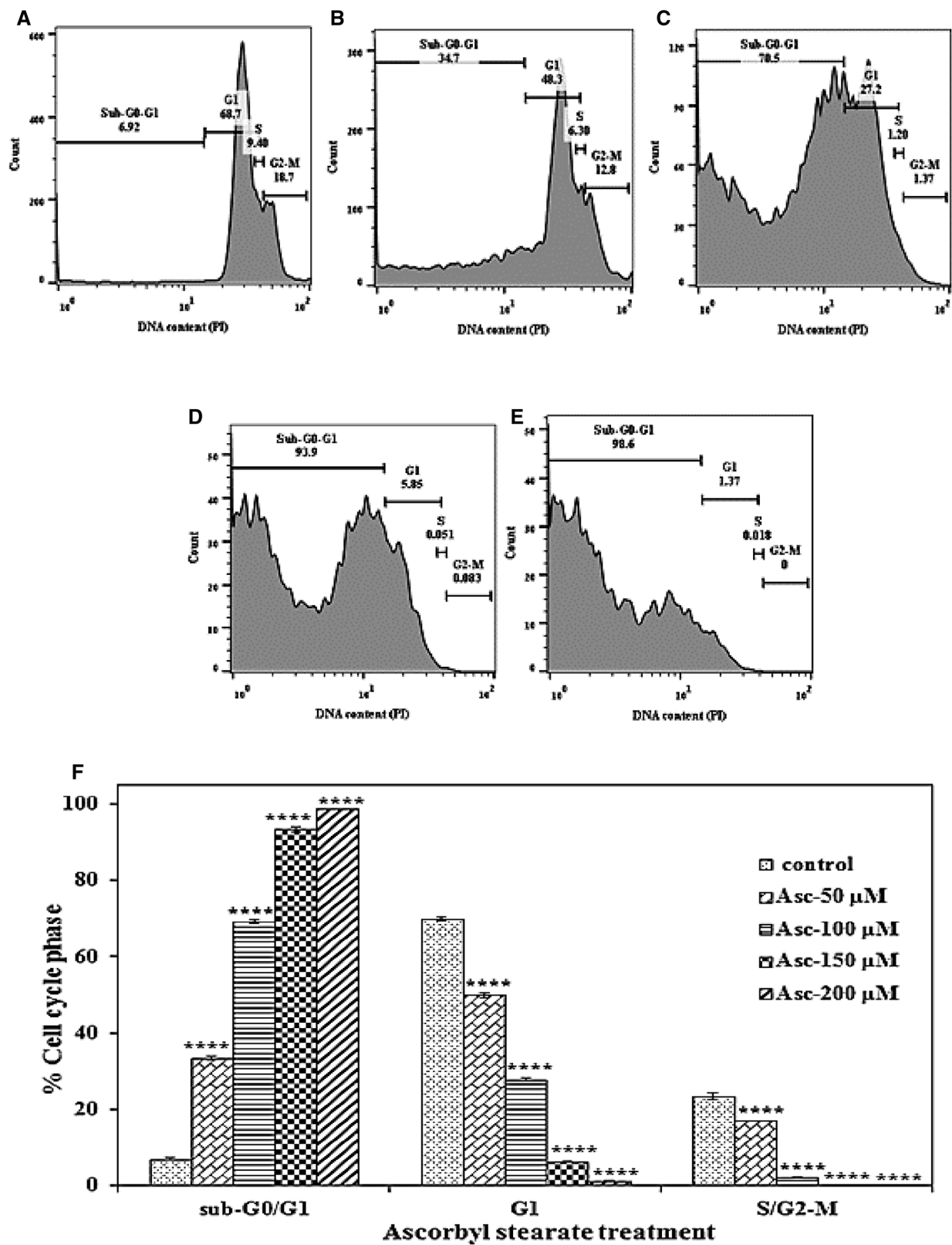


**Fig. 2** Effect of Asc-s on cell cycle distribution of HeLa cells. **a–e** Cells treated with various concentrations of Asc-s (0, 50, 100,150, and 200 μM) for 48 h were collected and stained with propidium iodide and analysed by flow cytometry. **f** Significant accumulation

of cells at sub-G0/G1 at 50, 100, 150, and 200 μM of Asc-s treatment was observed compared with control cells. Data represent mean ± SE of three independent experiments; values are significant at \*\*\*\* $p < 0.0001$

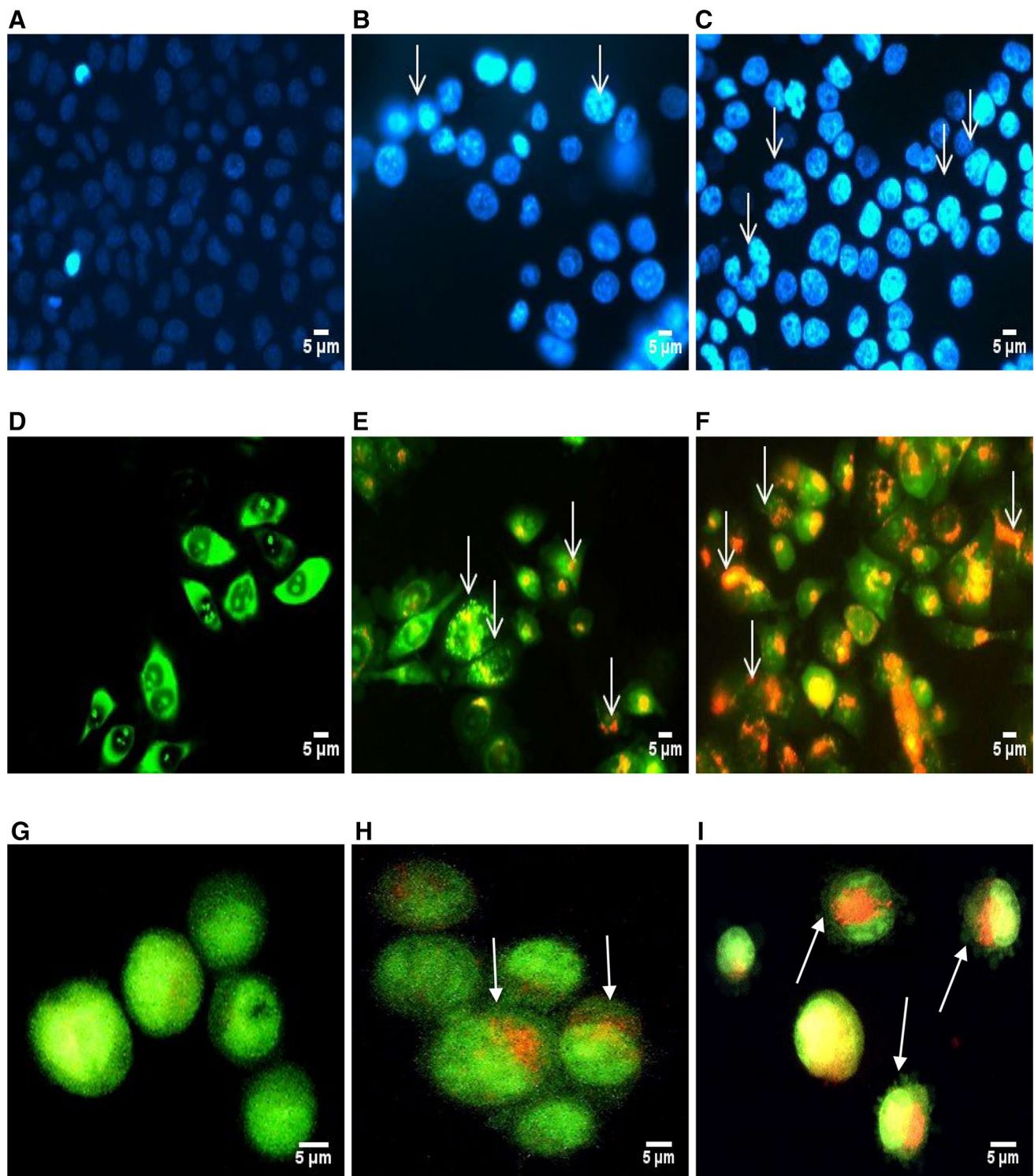
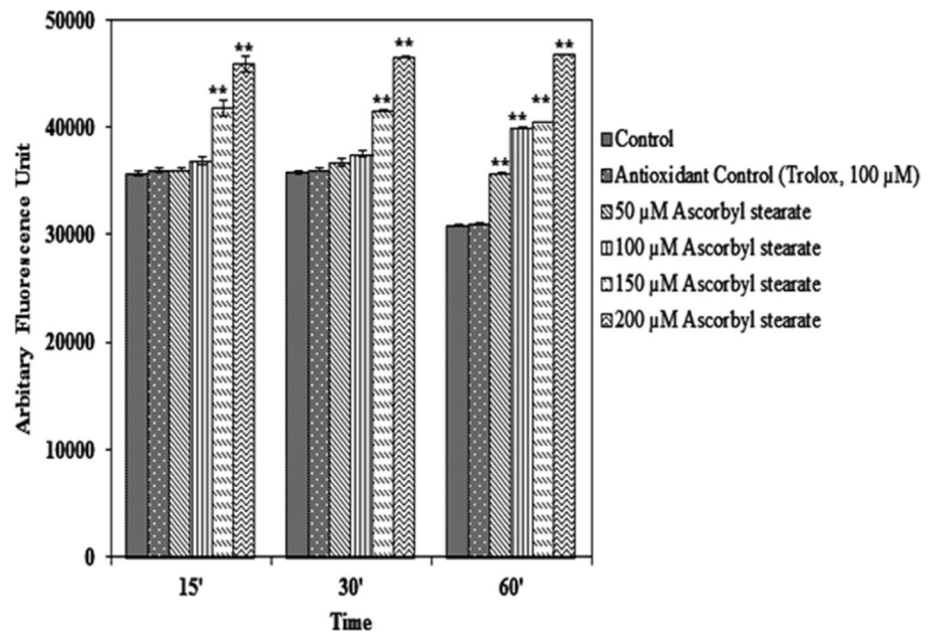


**Fig. 3** Pro-apoptotic effect of Asc-s on HeLa cells. **a** DAPI-stained control HeLa cells without blue fluorescence when treated with DMSO for 48 h, **b** DAPI-stained HeLa cells treated with 126  $\mu$ M Asc-s for 24 h, **c** DAPI-stained HeLa cells apoptotic bodies with bright blue fluorescence and more nuclear or chromatin condensation when treated with 126  $\mu$ M Asc-s for 48 h, arrows indicate apoptotic bodies of nuclear fragmentation and chromatin condensation (4 B and

4 C, respectively), **d, g** PI and AO stained control HeLa cells treated with DMSO for 48 h, **e, h** PI and AO stained HeLa cells treated with 126  $\mu$ M Asc-s for 24 h, showed early apoptosis features represented as intercalated acridine orange (bright green) amongst the fragmented DNA (arrows), **f, i** PI and AO stained HeLa cells treated with 126  $\mu$ M of Asc-s for 48 h, depicts blebbing and nuclear margination noticeable at 48 h treatment (arrows)

**Fig. 4** Effect of Asc-s treatment on ROS levels in HeLa cells measured by DCFH2 method. Dose-dependent increase in ROS levels was observed at 15–60 min of 50–200  $\mu\text{M}$  Asc-s treatment. Antioxidant control comprises of (Trolox, 100  $\mu\text{M}$ ) with 126  $\mu\text{M}$  Asc-s treatment followed by DCF-DA staining. Data represent mean  $\pm$  SE ( $n=3$ ). Values are significant at  $**p < 0.01$



### Effect of Asc-s on cell-membrane permeability and membrane fluidity

Cell-membrane permeability reflects the degree of the cell-membrane injury, as indicated by corresponding PI permeability of cell membrane. A dose-dependent increase in PI uptake ( $p < 0.01$ ) corresponding to Asc-s doses (0, 50, 100, 150, and 200  $\mu\text{M}$ ) was observed suggesting changes in permeability of HeLa cells for intracellular uptake of Asc-s (Fig. 6b). Furthermore, a dose-dependent increase in anisotropy values ( $p < 0.001$ ) was observed on treatment with Asc-s as suggesting a decrease in membrane fluidity of cells (Fig. 6a). These results clearly demonstrate that Asc-s treatment brought about alterations in membrane permeability and fluidity in HeLa cells.

### Metabolism of Asc-s in HeLa cells

Exposure of HeLa cells to 126  $\mu\text{M}$  Asc-s for 12, 24, and 48 h resulted in intracellular permeation of Asc-s. The intracellular Asc-s levels decreased with increase in exposure time period (Table 1). Simultaneously, there was the presence of ascorbate and stearate moieties at different time intervals in due metabolism of Asc-s by esterase of HeLa cells. The result clearly demonstrates that Asc-s enters HeLa cells and it was metabolized to ascorbate and stearate moieties by esterases present in HeLa cells.

### Effect of Asc-s on fatty acid composition of HeLa cells

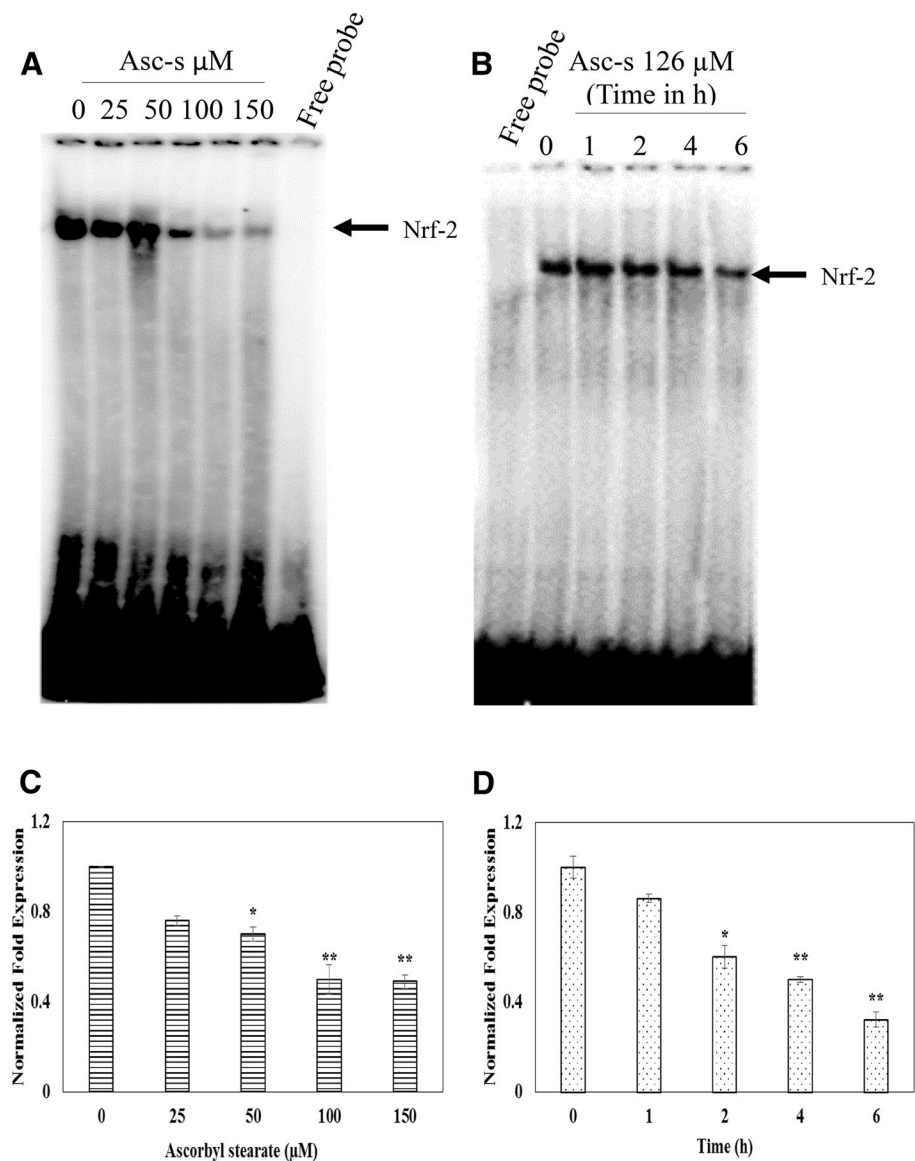
Fatty acid composition of HeLa cells at different time intervals of 12, 24, and 48 h after treatment with 126  $\mu\text{M}$  Asc-s is presented in Table 2. Stearic acid content increased by 9.4-fold by 48 h of Asc-s treatment due to break down of Asc-s to stearic acid and ascorbate. Oleic acid content was also increased (3.37-fold) in HeLa on treatment with Asc-s for 48 h ( $p < 0.001$ ). Furthermore, 3.3-fold increase in the ratio of saturated to unsaturated fatty acids was observed in HeLa cells by 48 h of Asc-s treatment.

### Immunoblot and RT-qPCR analysis of LC3 and autophagy in Asc-s treated HeLa Cells

Immunoblot analysis of 0–200  $\mu\text{M}$  Asc-s treated HeLa cell lysate showed a drastic  $\sim$ threefold dose-dependent decrease ( $p < 0.01$ ) in LC3-I levels and profound  $\sim$ 200-fold increase ( $p < 0.01$ ) in LC3-II level as compared to untreated HeLa cells control, which is an indication of autophagosomes formation on Asc-s treatment to HeLa cells (Fig. 7 a–c). RT-PCR analysis of 0–200  $\mu\text{M}$  Asc-s-treated HeLa cell lysate showed  $\sim$ 4.3-fold increase in LC3 mRNA expression with respect to control cells, in a dose-dependent increase format ( $p < 0.05$ ) (Fig. 7d).



**Fig. 5** Nrf-2 levels in HeLa cells were probed by EMSA and RT-qPCR. EMSA profile of Nrf-2 **a** presence and absence of Asc-s at concentration dependent for 6 h incubation, **b** time-dependent manner when treated with 100  $\mu\text{M}$  Asc-s, **c, d** dose-dependent decrease in qRT-PCR profile of Nrf-2 mRNA levels in HeLa cell lysate treated with Asc-s (0–200  $\mu\text{M}$ ) for 6 h and in HeLa cell lysate treated with 126  $\mu\text{M}$  Asc-s for 0–6 h, when compared with untreated HeLa cells. Data represent mean  $\pm$  SE ( $n = 3$ ). Values are significant at  $*p < 0.5$  and  $**p < 0.01$



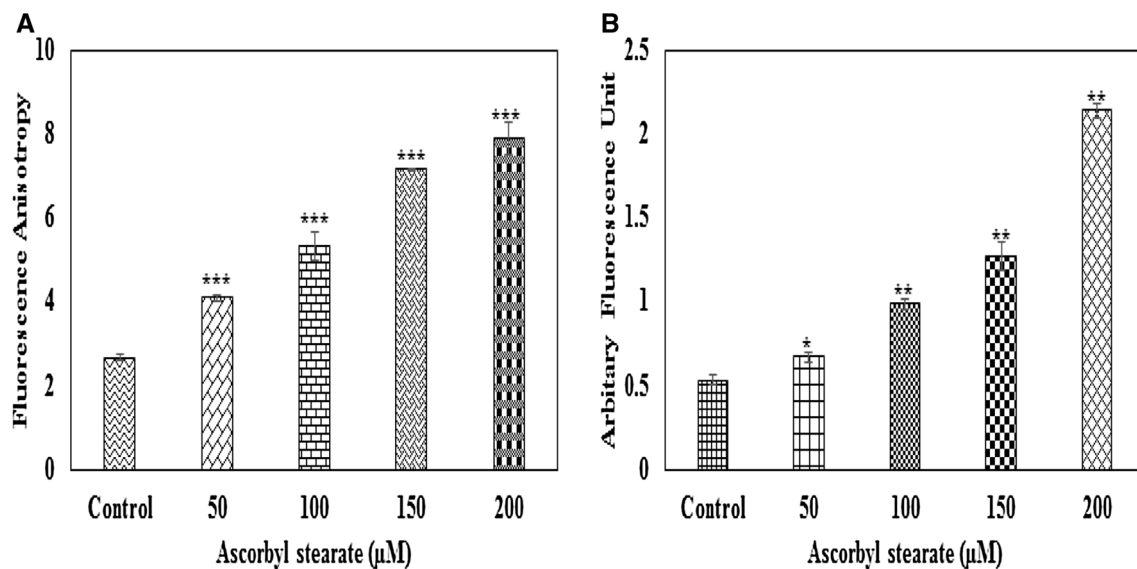
### Effect of Asc-s in splenic lymphocytes

Figure 8 depicts the effect of Asc-s on murine splenic lymphocytes. Lymphocytes on treatment with Asc-s were stained with PI to address toxicity of this compound. Results depict non-significant percentage of apoptosis and presence of healthy cells in G1 phase of cell cycle. The results show non-toxicity of Asc-s on splenic lymphocytes.

### Discussion

Ascorbic acid (AA) an essential nutrient and antioxidant has diverse physiological functions. High doses of AA were advocated for treatment of cancer in 1970s. However, randomized controlled clinical trials produced inconsistent

results due to poor bioavailability and efficacy of AA (Wilson et al. 2014). At physiological concentrations, AA do not have any effect on cancer cells, hence mega doses of AA was given to treat cancer patients (Chen et al. 2007). However, oral administration of high doses of AA compromised the absorption and plasma concentration due to elimination of excess AA by the kidney (Wilson et al. 2014). The clinical and pharmacokinetics studies showed that AA concentrations in plasma and tissues were tightly controlled (Graumlich et al. 1997). To overcome the poor absorption and bioavailability of AA during oral dosing, intravenous administration of high doses of AA was promoted as complimentary and alternate therapy to cure certain cancers (Padayatty et al. 2010). Despite the ambiguity on anti-cancer propensity of AA, a number of derivatives were being synthesized and their anti-cancer potential



**Fig. 6** Effect of different concentrations of Asc-s on membrane permeability and membrane fluidity of HeLa cells. **a** Anisotropic values for 1,6-diphenyl-1,3,5-hexatriene (DPH) stained HeLa cell showing decreased membrane fluidity on treatment with 0, 50, 100, 150, and 200 μM of Asc-s for 48 h, **b** fluorescence values of propidium

iodide stained HeLa cell indicating increased membrane permeability treated with 0, 50, 100, 150, and 200 μM of Asc-s for 48 h. Data represent mean  $\pm$  SE ( $n=3$ ). Values are significant at \* $p < 0.05$ , \*\* $p < 0.01$ , \*\*\* $p < 0.001$

has been investigated in a number of malignant cell lines (Shibuya et al. 2012; Bordignon et al. 2013). This study reports the possible mechanism of action of Asc-s on anti-proliferative and apoptotic effect in human cervical cancer cells (HeLa). Few studies have been conducted on the anti-cancer effects of AA on human cervical cancer cells. A concentration of 7–10 mM of AA is reported to be effective in inducing cytotoxicity and cell death in cervical cancer cells (Roberts et al. 2015). In our study, Asc-s treatment dose-dependently inhibited the proliferation of HeLa cells at micro molar concentration (Fig. 1) with an  $IC_{50}$  value of 126 μM after 48 h of treatment. Cell-cycle analysis showed that Asc-s inhibited cell-cycle progression at sub-G<sub>0</sub>/G<sub>1</sub> phase resulting in apoptosis of HeLa cells (Fig. 2). Furthermore, Asc-s treatment-induced apoptosis characterized by condensation of cytoplasm, loss of plasma membrane microvilli, fragmentation of nucleus, and extensive degradation of

chromosomal DNA in HeLa cells, which were visualized by DAPI (Rabelo et al. 2012; Wahab et al. 2009), propidium, and acridine orange staining. HeLa cells stained with propidium iodide analysed with Partec flow cytometer showed DNA damage and cell death. An increase in cell-membrane permeability (Fig. 6a, b) and alteration in membrane fluidity observed due to Asc-s treatment might facilitate easy passage of Asc-s through the cell membrane and even intracellular membranes, such as the mitochondria (Rasmussen et al. 2010). The metabolism studies showed that Asc-s easily permeates through cell membrane and it is partially metabolized to ascorbyl radical and stearate moieties by intracellular esterases in HeLa cells (Tables 1 and 2). Our findings are in agreement with earlier reports that L-ascorbic acid 2-phosphate-6-palmitate (Asc2P6P) enter PC12 cells and converted to ascorbyl radical (Du et al. 2003). Ascorbyl radical thus formed might generate  $H_2O_2$  by Fenton reaction in cells which can further induce cell death as reported earlier (Chen et al. 2007). The formation of  $H_2O_2$  is further evidenced by decrease in Nrf-2 signalling during Asc-s treatment at concentration and time-dependent manner (Fig. 5). However, Asc-s treatment showed no significant toxicity to normal lymphocytes (Fig. 8). HeLa cells express higher level of Nrf-2 an oxidative stress responsive gene which regulates superoxide dismutase,  $\gamma$ -glutamylcysteine synthetase ( $\gamma$ -GCS), and cysteine membrane transport (system x-c), thus playing a role in the defence against oxidative stress by neutralizing compounds capable of generating ROS (Kotlo et al. 2003). In our study, Asc-s decreased the

**Table 1** Concentration of Asc-s and its metabolites at different time intervals in HeLa cells after exposure to 126 μM Asc-s

Treatment time (h)	Ascorbyl stearate (μmole/10 <sup>6</sup> cells)	Ascorbate (μmole/10 <sup>6</sup> cells)	Stearic acid (μmole/10 <sup>6</sup> cells)
0	0.062 $\pm$ 0.001	–	–
12	0.047 $\pm$ 0.0002	0.055 $\pm$ 0.0002	0.03 $\pm$ 0.001
24	0.033 $\pm$ 0.001	0.045 $\pm$ 0.03	0.025 $\pm$ 0.0001
48	0.026 $\pm$ 0.002	0.039 $\pm$ 0.002	0.02 $\pm$ 0.001

Values are described as mean  $\pm$  SE ( $n=3$ )

**Table 2** Effect of Asc-s on fatty acid composition of HeLa cells at different time intervals

Fatty acids	Control	Asc-s 126 $\mu$ M		
		12 h	24 h	48 h
Myristic acid	1.07 $\pm$ 0.06	1.41 $\pm$ 0.06	0.80 $\pm$ 0.05	1.10 $\pm$ 0.09
Palmitic acid	0.46 $\pm$ 0.16	2.28 $\pm$ 0.33	5.73 $\pm$ 0.19	6.28 $\pm$ 0.09
Hexadecenoic acid	40.29 $\pm$ 0.25	41.13 $\pm$ 0.19	32.98 $\pm$ 0.5	35.1 $\pm$ 0.40
Stearic acid	0.30 $\pm$ 0.07	0.95 $\pm$ 0.04*	1.62 $\pm$ 0.03**	2.82 $\pm$ 0.40**
Oleic acid	0.08 $\pm$ 0.03	1.07 $\pm$ 0.02*	1.99 $\pm$ 0.02**	2.47 $\pm$ 0.30**
Linoleic acid	29.0 $\pm$ 0.21	35.38 $\pm$ 0.17	30.85 $\pm$ 0.3	28.96 $\pm$ 0.4
$\alpha$ -Linolenic acid	1.34 $\pm$ 0.02	2.20 $\pm$ 0.02	1.91 $\pm$ 0.05	1.87 $\pm$ 0.05
Eicosenoic acid	0.58 $\pm$ 0.02	0.19 $\pm$ 0.02	0.23 $\pm$ 0.01	0.29 $\pm$ 0.10
Eicosadienoic acid	0.28 $\pm$ 0.02	0.46 $\pm$ 0.03	0.35 $\pm$ 0.02	0.43 $\pm$ 0.03
Eicosatrienic acid	0.13 $\pm$ 0.002	0.04 $\pm$ 0.001	0.26 $\pm$ 0.03	0.05 $\pm$ 0.01
Arachidonic acid	18.4 $\pm$ 0.08	8.88 $\pm$ 0.12	14.58 $\pm$ 0.4	14.2 $\pm$ 0.5
Eicosapentaenic acid	3.99 $\pm$ 0.18	4.0 $\pm$ 0.06	4.72 $\pm$ 0.03	3.54 $\pm$ 0.07
Erucic acid	1.23 $\pm$ 0.04	1.8 $\pm$ 0.01	1.51 $\pm$ 0.01	2.44 $\pm$ 0.4
Saturated/unsaturated fatty acid ratio	0.03 $\pm$ 0.003	0.04 $\pm$ 0.004	0.96 $\pm$ 0.001***	0.1 $\pm$ 0.003***

Values are mean  $\pm$  SE ( $n=3$ ); values are significant at \* $p < 0.05$ ; \*\* $p < 0.01$ ; \*\*\* $p < 0.001$

nuclear translocation of Nrf-2 and thus facilitated the formation of  $H_2O_2$  (Kenific and Debnath 2015). Furthermore, the stearic acid formed by cleavage of Asc-s-induced cell death due to change in membrane fluidity. It is suggested that fatty acid moiety in monocylated ascorbic acid viz., ascorbyl stearate and ascorbyl palmitate might affect the balance in the hydrophobicity/hydrophilicity and enhance intracellular permeability of cell membrane leading to breakdown of cell membrane and cell death (Kageyama et al. 1991; Kato et al. 2011). Moreover, our observation is in agreement with reports that saturated fatty acid such as palmitate and stearate can induce cell death/apoptosis as suggested by Evans et al. 2009, indicating the role of the fatty acid moiety in inducing cell death of HeLa cells. In human cells, stearic acid is converted to monounsaturated fatty acid oleic acid by the enzyme stearoyl-CoA desaturase (Sampath and Ntambi 2005). In agreement with earlier reports, a significant increase in oleic acid content was observed in HeLa cells on treatment with Asc-s (Table 2). The cellular ratio of oleic to stearic acids has been reported to modulate membrane fluidity and signal transduction that can, in turn, trigger cell for apoptosis (Kasai et al. 1998; Sun et al. 2003). Furthermore, oleic acid is also reported to inhibit proliferation and induce apoptosis of different carcinoma cells. The oleic acid expression functioning as autophagosome marker present in autophagosomal membrane could be correlated to robust functioning of SCD1 (Ogasawara et al. 2014). Since SCD1 is a pre-requisite protein for autophagy, increase in oleic acid content might lead to over expression of SCD1 and hence triggering autophagy, which is in correlation with the earlier reports (Carrillo et al. 2012; Ogasawara et al. 2014). There

is a link suggesting Nrf-2 promoting autophagy (Kenific and Debnath 2015), which further supports autophagy initiation resulting from reduced Nrf-2 nuclear translocation on Asc-s treatment. Thus, the cell death induced by Asc-s in HeLa cells could be attributed to increase in membrane permeability, decrease in membrane fluidity, and increase in ROS level and also due to autophagy in HeLa cells.

Finally, we hypothesize that there are two main pathways by which Asc-s may affect the cancer cells (i) the ascorbyl radical can cause cell death by forming  $H_2O_2$  and (ii) saturated fatty acid stearic acid and monounsaturated fatty acid oleic acid moieties can also induce autophagy by altering cellular membrane permeability and fluidity in HeLa cancer cells. Furthermore, the propensity of Asc-s could be attributed to combined cytotoxic effect of ascorbyl radical and stearoyl moiety on HeLa cells.

## Conclusion

In summary, our results clearly demonstrate that at micromolar concentration Asc-s-induced cell death through modulation of membrane permeability, membrane fluidity, increase in ROS formation, and decrease in Nrf-2 nuclear translocation thereby formation of ROS in HeLa cells leading to autophagosomes formation and autophagy. To our knowledge, this first report on possible mechanism of action of Asc-s on HeLa cancer cells. Our findings suggest that Asc-s could be an effective anti-cancer compound in addition to being a food stabiliser. These assets could be useful

**Fig. 7** Immunoblot and real-time PCR profile of autophagy protein LC3. **a** HeLa cells were treated with Asc-s (0–200  $\mu$ M) for 48 h. Cell lysates were processed for immunoblot study to detect LC3 and  $\beta$ -actin as loading control. **b** Dose-dependent decrease in LC3-I levels was observed in HeLa cell lysate treated with Asc-s (0–200  $\mu$ M) for 48 h when compared with untreated HeLa cells, **c** dose-dependent increase in LC3-II levels in HeLa cell lysate treated with Asc-s (0–200  $\mu$ M) for 48 h when compared with untreated HeLa cells, **d** dose-dependent increase in RT-qPCR profile of LC3 mRNA levels in HeLa cell lysate treated with Asc-s (0–200  $\mu$ M) for 48 h when compared with untreated HeLa cells. Data represent mean  $\pm$  SE ( $n=3$ ). Values are significant at \* $p < 0.5$  and \*\* $p < 0.01$

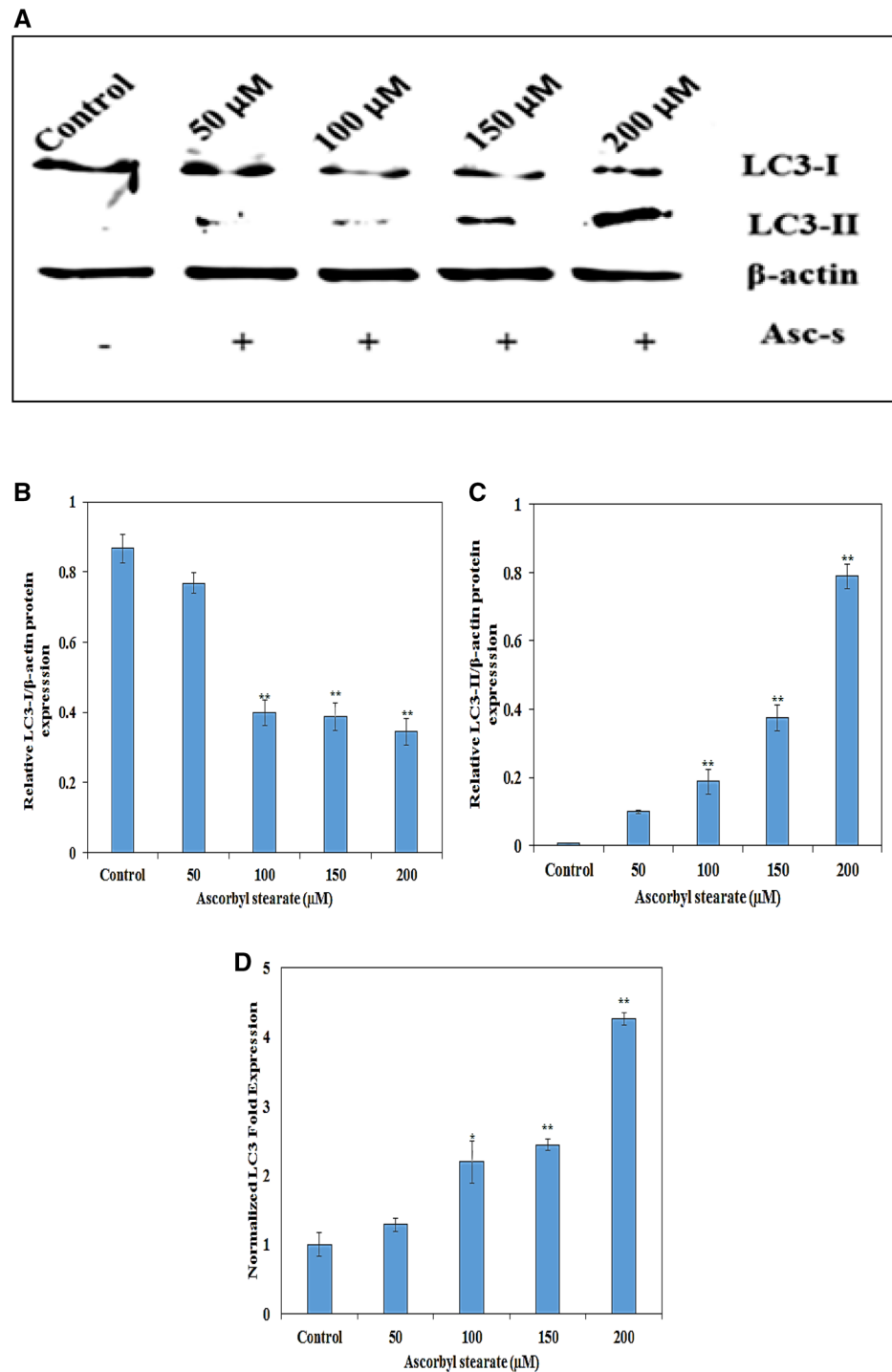
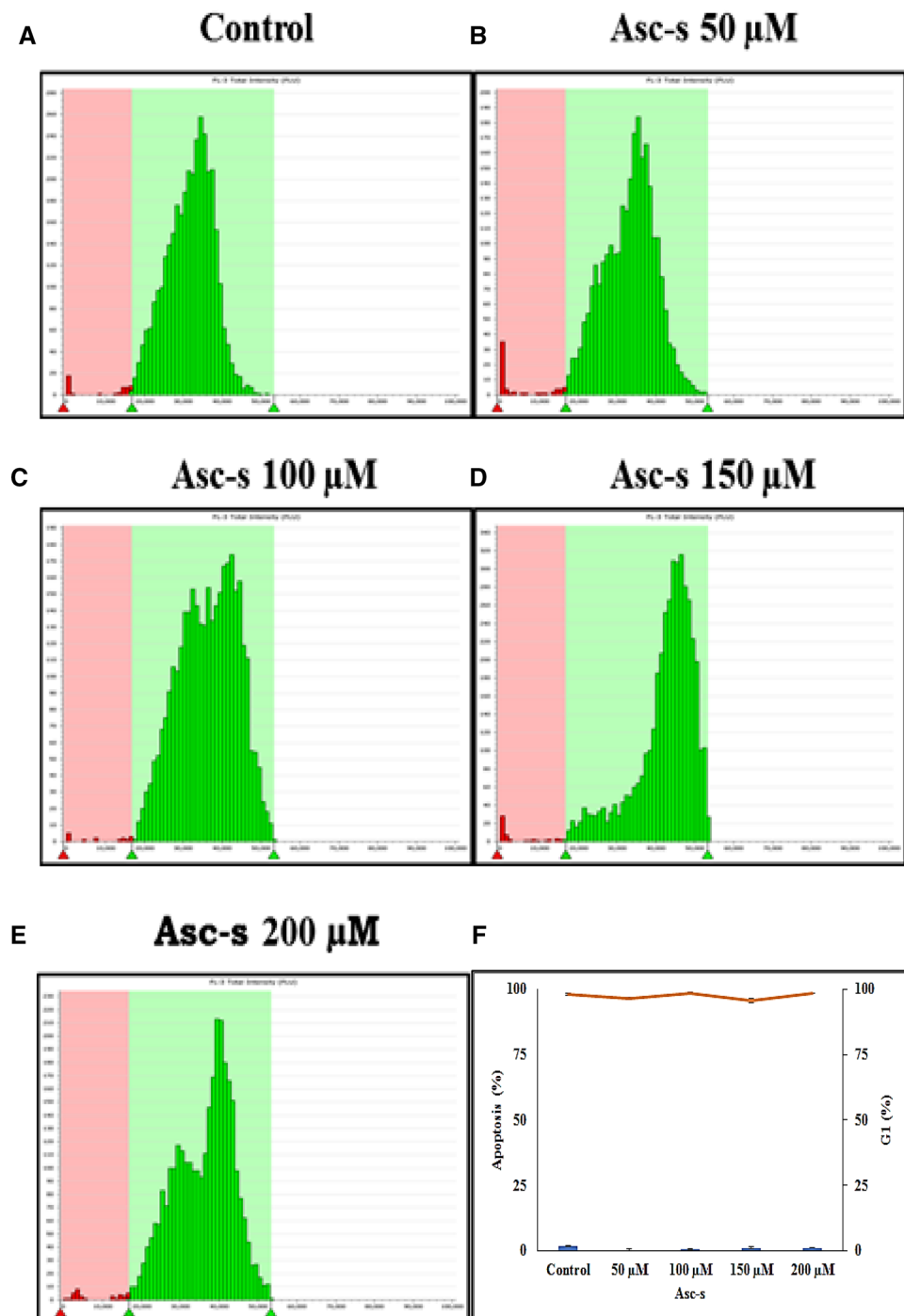




**Fig. 8** Effect of Asc-s on murine splenic lymphocytes. **a–e** Histogram depicting the effect of different concentrations of Asc-s on murine splenic lymphocytes investigated by propidium iodide staining and analysed by high content screening instrument (Acumen Celistra) from TTP Labtech, UK. **f** Bar diagram illustrates significant data point mean  $\pm$  SE of three independent experiments. No cell death of splenic lymphocytes on treatment with different concentrations of Asc-s



in health foods/nutraceuticals to restrain the cancer growth. However, further studies are warranted to test its efficacy in human subjects.

**Acknowledgements** The authors thank Prof. Ram Rajshekar, Director CSIR CFTRI., Mysore for encouragement in present study. The authors also thank Dr. S. Chattopadhyay, Associate Director,

Bioscience group and Head, Radiation Biology Health Sciences Division, B.A.R.C., Mumbai for permitting to carry out flow-cytometry related analysis. The authors express gratitude to Dr. Deepak Sharma and Dr. Santosh Kumar Sandur for providing lab facilities at Radiation Biology Health Sciences Division, B.A.R.C., Mumbai for conducting experiments. Mr. Shirish D. Mane, UGC-CSIR JRF, gratefully acknowledges the financial assistance from University Grant Commission (U.G.C.), New Delhi, in carrying out the research.

**Funding** This research did not receive any specific grant from funding agencies in the public, commercial, or not-for-profit sectors. Authors' contributions. SDM and KAN conceived and designed the experiments, SDM performed the experiments, the data were analysed by SDM and KAN.

## Compliance with ethical standards

**Conflict of interest** The authors declare that they have no competing interests.

## References

- Bhatla N, Lal N, Bao Y-P et al (2008) A meta-analysis of human papillomavirus type-distribution in women from South Asia: implications for vaccination. *Vaccine* 26:2811–2817. <https://doi.org/10.1016/j.vaccine.2008.03.047>
- Bordignon B, Chiron J, Fontés M (2013) Ascorbic acid derivatives as a new class of antiproliferative molecules. *Cancer Lett* 338:317–327. <https://doi.org/10.1016/j.canlet.2013.06.015>
- Bruni L, Barrionuevo-Rosas L, Albero G et al (2015) Human papillomavirus and related diseases in the world. ICO Information Centre on HPV and Cancer (HPV Information Centre)
- Carrillo C, Cavia dM, Alonso-Torre SR (2012) Antitumor effect of oleic acid; mechanisms of action. A review. *Nutr Hosp* 27:1860–1865. <https://doi.org/10.3305/nh.2012.27.6.6010>
- Checker R, Sharma D, Sandur SK et al (2010) Plumbagin inhibits proliferative and inflammatory responses of T cells independent of ROS generation but by modulating intracellular thiols. *J Cell Biochem* 110:1082–1093. <https://doi.org/10.1002/jcb.22620>
- Chen Q, Espey MG, Sun AY et al (2007) Ascorbate in pharmacologic concentrations selectively generates ascorbate radical and hydrogen peroxide in extracellular fluid in vivo. *Proc Natl Acad Sci USA* 104:8749–8754. <https://doi.org/10.1073/pnas.0702854104>
- Cleaver G (2015) Analysis of foods using HPLC with evaporative light scattering detection. <http://www.agilent.com/cs/library/applications/5990-9456EN>. Accessed 10 Feb 2018
- Clements CM, McNally RS, Conti BJ et al (2006) DJ-1, a cancer- and Parkinson's disease-associated protein, stabilizes the antioxidant transcriptional master regulator Nrf2. *Proc Natl Acad Sci USA* 103:15091–15096. <https://doi.org/10.1073/pnas.0607260103>
- Du C-B, Liu J-W, Su W et al (2003) The protective effect of ascorbic acid derivative on PC12 cells: Involvement of its ROS scavenging ability. *Life Sci* 74:771–780. <https://doi.org/10.1016/j.lfs.2003.07.014>
- Evans LM, Cowey SL, Siegal GP, Hardy RW (2009) Stearate preferentially induces apoptosis in human breast cancer cells. *Nutr Cancer* 61:746–753. <https://doi.org/10.1080/01635580902825597>
- Folch J, Lees M, Sloane Stanley GH (1957) A simple method for the isolation and purification of total lipids from animal tissues. *J Biol Chem* 226:497–509
- Graumlich JF, Ludden TM, Conry-Cantilena C et al (1997) Pharmacokinetic model of ascorbic acid in healthy male volunteers during depletion and repletion. *Pharm Res* 14:1133–1139. <https://doi.org/10.1023/A:1012186203165>
- Jemal A, Bray F, Center MM et al (2011) Global cancer statistics. *CA Cancer J Clin* 61:69–90. <https://doi.org/10.3322/caac.20107>
- Kageyama K, Onoyama Y, Kimura M et al (1991) Enhanced inhibition of DNA synthesis and release of membrane phospholipids in tumour cells treated with a combination of acylated ascorbate and hyperthermia. *Int J Hyperthermia* 7:85–91. <https://doi.org/10.3109/02656739109004979>
- Kar R, Singha PK, Venkatachalam MA, Saikumar P (2009) A novel role for MAP1 LC3 in nonautophagic cytoplasmic vacuolation death of cancer cells. *Oncogene* 28:2556. <https://doi.org/10.1038/onc.2009.118>
- Kasai T, Ohguchi K, Nakashima S et al (1998) Increased activity of oleate-dependent type phospholipase D during actinomycin D-induced apoptosis in Jurkat T cells. *J Immunol* 161:6469–6474
- Kato S, Asada R, Kageyama K et al (2011) Anticancer effects of 6-o-palmitoyl-ascorbate combined with a capacitive-resistive electric transfer hyperthermic apparatus as compared with ascorbate in relation to ascorbyl radical generation. *Cytotechnology* 63:425–435. <https://doi.org/10.1007/s10616-011-9363-8>
- Kenific CM, Debnath J (2015) Cellular and metabolic functions for autophagy in cancer cells. *Trends Cell Biol* 25:37–45. <https://doi.org/10.1016/j.tcb.2014.09.001>
- Kotlo KU, Yehiely F, Efimova E et al (2003) Nrf2 is an inhibitor of the Fas pathway as identified by Achilles' Heel Method, a new function-based approach to gene identification in human cells. *Oncogene* 22:797. <https://doi.org/10.1038/sj.onc.1206077>
- Levine M, Conry-Cantilena C, Wang Y et al (1996) Vitamin C pharmacokinetics in healthy volunteers: evidence for a recommended dietary allowance. *Proc Natl Acad Sci USA* 93:3704–3709
- Lu X, He G, Yu H et al (2010) Colorectal cancer cell growth inhibition by linoleic acid is related to fatty acid composition changes. *J Zhejiang Univ Sci B* 11:923–930
- Morrison WR, Smith LM (1964) Preparation of fatty acid methyl esters and dimethylacetals from lipids with boron fluoride-methanol. *J Lipid Res* 5:600–608
- Mountzios G, Soultati A, Pectasides D et al (2013) Developments in the systemic treatment of metastatic cervical cancer. *Cancer Treat Rev* 39:430–443. <https://doi.org/10.1016/j.ctrv.2012.05.009>
- Naidu KA, Fang Q, Naidu KA et al (2007) P53 enhances ascorbyl stearate-induced G2/M arrest of human ovarian cancer cells. *Anticancer Res* 27:3927–3934
- Nandakumar A, Ramnath T, Chaturvedi M (2009) The magnitude of cancer cervix in India. *Indian J Med Res* 130:219
- Ogasawara Y, Itakura E, Kono N et al (2014) Stearoyl-CoA desaturase 1 activity is required for autophagosome formation. *J Biol Chem* 289:23938–23950. <https://doi.org/10.1074/jbc.M114.591065>
- Padayatty SJ, Sun AY, Chen Q et al (2010) Vitamin C: intravenous use by complementary and alternative medicine practitioners and adverse effects. *PLoS One* 5:e11414. <https://doi.org/10.1371/journal.pone.0011414>
- Patwardhan RS, Checker R, Sharma D et al (2013) Involvement of ERK-Nrf-2 signaling in ionizing radiation induced cell death in normal and tumor cells. *PLoS One* 8:e65929. <https://doi.org/10.1371/journal.pone.0065929>
- Rabelo L, Monteiro N, Serquiz R et al (2012) A lactose-binding lectin from the marine sponge *Cinachyrella apion* (Cal) induces cell death in human cervical adenocarcinoma cells. *Mar Drugs* 10:727–743. <https://doi.org/10.3390/md10040727>
- Rasmussen N, Andersen JH, Jespersen H et al (2010) Effect of free fatty acids and lysolipids on cellular uptake of doxorubicin in human breast cancer cell lines. *Anticancer Drugs* 21:674–677. <https://doi.org/10.1097/CAD.0b013e32833c2cf7>
- Roberts BM, Fullerton DR, Elliott SL (2015) High concentrations of L-ascorbic acid (Vitamin C) induces apoptosis in a human cervical cancer cell line (HeLa) through the intrinsic and extrinsic pathways. *Bios* 86:134–143. <https://doi.org/10.1893/BIOS-D-14-00019.1>
- Sampath H, Ntambi JM (2005) The fate and intermediary metabolism of stearic acid. *Lipids* 40:1187–1191. <https://doi.org/10.1007/s11745-005-1484-z>
- Sawant RR, Vaze O, D'Souza GG et al (2011) Palmitoyl ascorbate-loaded polymeric micelles: cancer cell targeting and

- cytotoxicity. *Pharm Res* 28:301–308. <https://doi.org/10.1007/s11095-010-0242-3>
- Sharma D, Sandur SK, Rashmi R et al (2010) Differential activation of NF- $\kappa$ B and nitric oxide in lymphocytes regulates in vitro and in vivo radiosensitivity. *Mutat Res Genet Toxicol Environ Mutagen* 703:149–157. <https://doi.org/10.1016/j.mrgentox.2010.08.010>
- Shibuya S, Kinoshita K, Shimizu T (2012) Protective effects of vitamin C derivatives on skin atrophy caused by Sod1 deficiency. In: *Handbook of diet, nutrition and the skin*. Springer, New York, pp 350–364. [https://doi.org/10.3920/978-90-8686-729-5\\_21](https://doi.org/10.3920/978-90-8686-729-5_21)
- Sun Y, Hao M, Luo Y et al (2003) Stearoyl-CoA desaturase inhibits ATP-binding cassette transporter A1-mediated cholesterol efflux and modulates membrane domain structure. *J Biol Chem* 278:5813–5820. <https://doi.org/10.1074/jbc.M208687200>
- Trumpi K, Egan DA, Vellinga TT et al (2015) Paired image-and FACS-based toxicity assays for high content screening of spheroid-type tumor cell cultures. *FEBS open bio* 5:85–90. <https://doi.org/10.1016/j.fob.2015.01.003>
- Wahab A, Ibrahim S, Abdul AB et al (2009) In vitro ultramorphological assessment of apoptosis induced by zerumbone on (HeLa). *Biomed Res Int*. <https://doi.org/10.1155/2009/769568>
- Wilson MK, Baguley BC, Wall C et al (2014) Review of high-dose intravenous vitamin C as an anticancer agent. *Asia Pac J Clin Oncol* 10:22–37. <https://doi.org/10.1111/ajco.12173>